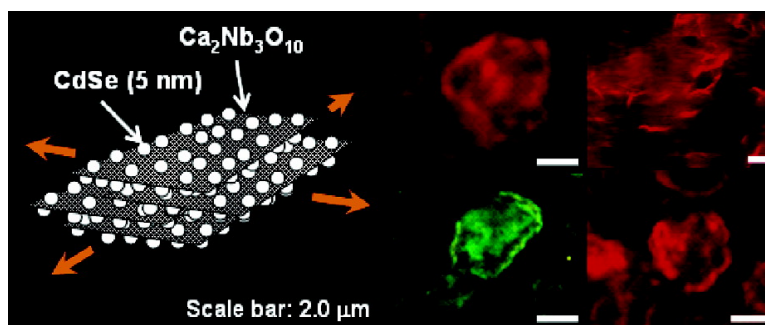Article

Planar Polarized Light Emission from CdSe Nanoparticle Clusters

Jin Young Kim, Hiroki Hiramatsu, and Frank E. Osterloh

More About This Article

Additional resources and features associated with this article are available within the HTML version:

- Supporting Information
- Links to the 4 articles that cite this article, as of the time of this article download
- Access to high resolution figures
- Links to articles and content related to this article
- Copyright permission to reproduce figures and/or text from this article

View the Full Text HTML

Planar Polarized Light Emission from CdSe Nanoparticle Clusters

Jin Young Kim, Hiroki Hiramatsu, and Frank E. Osterloh*

Contribution from the Department of Chemistry, University of California, Davis, California 95616

Received June 22, 2005; E-mail: osterloh@chem.ucdavis.edu

Abstract: This paper describes synthesis and optical properties of planar clusters of CdSe nanocrystals. The clusters emit linearly polarized light in the plane of the cluster. The emission wavelength of the clusters can be adjusted between 568 and 639 nm with the size of the CdSe nanocrystals. Planar CdSe microclusters were synthesized by reaction of trioctylphosphine oxide-coated CdSe/CdS nanocrystals with 3-aminopropylsilyl-modified $Ca_2Nb_3O_{10}$ nanosheets in THF. The clusters are 3.92 ± 1.18 μm length/width and 91 ± 37 nm thickness, and they consist of alternating layers of $Ca_2Nb_3O_{10}$ to which CdSe nanocrystals are attached with densities of 5300 ± 310 particles per side of a single $Ca_2Nb_3O_{10}$ sheet. The chemical inertness of the clusters in coordinating solvents suggests covalent interactions between the aminopropyl groups and CdSe nanocrystals. Upon excitation at $\lambda_{exc} = 400$ nm, the clusters emit green (568 nm), orange (589 nm), or red (639 nm) light, depending on the size of the CdSe crystals. The light is emitted preferentially in the cluster plane and it is linearly polarized along the cluster edges. Combined fluorescence microscopy and atomic force microscopy reveal that the directional emission efficiency depends linearly on the thickness of the clusters, which varies between 70 and 180 nm. The ability to manipulate the direction and polarization of the photoemission of CdSe nanoparticles via assembly into 2D structures is of interest for applications of these and similar structures in advanced optical materials and devices.

Introduction

The ability to generate, manipulate, and guide light over great length scales has revolutionized communication technology. The next step in achieving high-bandwidth optical communication systems lies in the miniaturization of optical processing devices. Nanocrystals of metal oxides and metal chalcogenides are ideal building blocks for such devices, because they have the necessary high optical index of refraction that is needed to guide light and their emission properties can be adjusted by changing the particle dimensions. SiO_2-,[1] CdS-,[2] CdSe-,[3] SnO_2-,[4] and ZnO-based[5,6] nanostructures, for example, have been demonstrated to efficiently transport planar light waves even when their sizes are smaller than the wavelength of the guided light. This makes such structures suitable as optical wiring for applications in photonic circuits.[7] For CdSe nanorods[8] and nanobelts,[3] and, separately, for ZnO[5] and InP[9] nanowires, it was

shown that, upon photoexcitation, these nanostructures are capable of directed emission of linearly polarized light. Depending on the system, the anisotropic emission properties are due to the intrinsic electronic structures of the particles,[3,8] or they result from the waveguiding properties of the interface between the nanomaterial and the surrounding matrix.[5,9]

While the morphologies of many inorganic nanomaterials and thus their optical properties can be adjusted via the conditions of synthesis, there is a practical limit on the achievable complexity of structures that are accessible by this approach. A much more versatile and more efficient way of tailoring the optical properties of nanomaterials is by chemical assembly into clusters. For example, we recently showed that axial CdSe microstructures could be generated by chemically linking CdSe nanocrystals to the surface of ZnO microcrystal rods.[10] The resulting ZnO−CdSe clusters were capable of directed light emission in the direction of the principal axis of the cluster (Figure 1) as result of a waveguiding effect at the cluster−air interface. Similar approaches were used by others to create hollow shells of CdSe or HgTe on the surface of SiO_2, glass, and polystyrene spheres (Figure 1).[11−14] In these structures the

(1) Tong, L. M.; Lou, J. Y.; Mazur, E. *Opt. Express* **2004**, *12* (6), 1025−1035.
(2) Barrelet, C. J.; Greytak, A. B.; Lieber, C. M. *Nano Lett.* **2004**, *4* (10), 1981−1985.
(3) Venugopal, R.; Lin, P.-I.; Liu, C.-C.; Chen, Y.-T. *J. Am. Chem. Soc.* **2005**, *127* (32), 11262−11268.
(4) Law, M.; Sirbuly, D. J.; Johnson, J. C.; Goldberger, J.; Saykally, R. J.; Yang, P. D. *Science* **2004**, *305* (5688), 1269−1273.
(5) Johnson, J. C.; Yan, H. Q.; Yang, P. D.; Saykally, R. J. *J. Phys. Chem. B* **2003**, *107* (34), 8816−8828.
(6) Huang, L. S.; Wright, S.; Yang, S. G.; Shen, D. Z.; Gu, B. X.; Du, Y. W. *J. Phys. Chem. B* **2004**, *108* (52), 19901−19903.
(7) Gibbs, W. W. *Sci. Am.* **2004**, *291*(5), 80−87.
(8) Hu, J. T.; Li, L. S.; Yang, W. D.; Manna, L.; Wang, L. W.; Alivisatos, A. P. *Science* **2001**, *292* (5524), 2060−2063.
(9) Wang, J. F.; Gudiksen, M. S.; Duan, X. F.; Cui, Y.; Lieber, C. M. *Science* **2001**, *293* (5534), 1455−1457.

(10) Kim, J. Y.; Osterloh, F. E. *J. Am. Chem. Soc.* **2005**, *127* (29), 10152−10153.
(11) Cha, J. N.; Bartl, M. H.; Wong, M. S.; Popitsch, A.; Deming, T. J.; Stucky, G. D. *Nano Lett.* **2003**, *3* (7), 907−911.
(12) Artemyev, M. V.; Woggon, U.; Wannemacher, R.; Jaschinski, H.; Langbein, W. *Nano Lett.* **2001**, *1* (6), 309−314.
(13) Fan, X. D.; Lonergan, M. C.; Zhang, Y. Z.; Wang, H. L. *Phys. Rev. B* **2001**, *64* (11), 115310.
(14) Shopova, S. I.; Farca, G.; Rosenberger, A. T.; Wickramanayake, W. M. S.; Kotov, N. A. *Appl. Phys. Lett.* **2004**, *85* (25), 6101−6103.
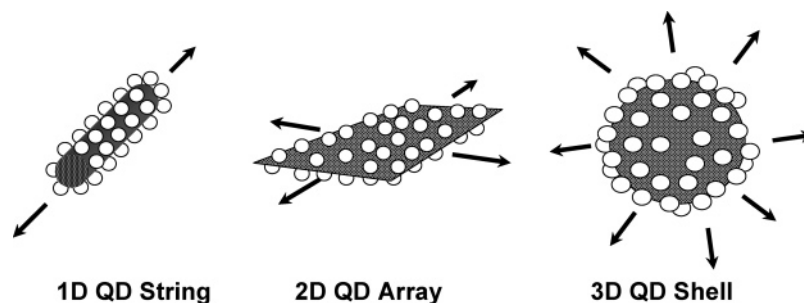
Figure 1. Structures and direction of light emission of CdSe quantum dot assemblies: $ZnO \cdot CdSe$ clusters (1D),[10] $Ca_2Nb_3O_{10} \cdot CdSe$ clusters (2D, this paper), and SiO_2 (PS)$\cdot CdSe$ (HgTe) clusters (3D).[11-14] PS = Polystyrene.

quantum dot photoemission couples to the eigenmodes of the optical cavity formed by the clusters. This coupling enables these "whispering gallery" resonators to function as microscale lasers.

In this paper, we show that by linking CdSe nanocrystals onto planar nanosheets derived from the layered perovskite $KCa_2Nb_3O_{10}$ it is possible to generate dispersible pseudo-two-dimensional arrays of CdSe nanocrystals, whose optical properties are modulated by the cluster shape. Upon photoexcitation, these platelike clusters emit linearly polarized light in the direction of the cluster plane at a wavelength that can be independently adjusted with the CdSe nanocrystal size. We report here on the synthesis and on the structures of this novel 2D-form of CdSe and on its anisotropic optical properties. The planar optical emission makes the CdSe clusters suitable for applications in advanced optical devices, e.g. in polarized light emitting diodes,[15] or as fillers for polymer composites with directional optical properties. Alternatively, the clusters could function as optical probes that could provide spatial and orientational information about their environment.

Experimental Section

3-Aminopropylsilyl (APS)-modified $[Ca_2Nb_3O_{10}]$ nanosheets were prepared as described earlier.[16] Trioctylphosphine oxide (TOPO)-coated CdSe/CdS core−shell nanocrystals were synthesized as described by Weller et al.[17] Tetrahydrofuran (THF) was dried over sodium benzophenone and distilled under nitrogen. Chloroform was used as received. Powder X-ray spectra were collected on a Scintag XDS 2000 powder X-ray diffractometer using Cu−Kα radiation. Infrared spectra were taken on a Mattson Galaxy Series FTIR 3000 spectrometer using KBr pellets. Atomic force micrographs (AFM) were obtained using a Nanoscope III Digital Instruments multimode atomic force microscope. The instrument was operated in tapping mode using Si probes (150 kHz, 5 N m). UV/vis spectra were recorded in standard quartz cuvettes using a Hewlett-Packard 8450A UV/vis spectrometer. Fluorescence spectra were recorded in standard quartz cuvettes using a Jobin-Ivon Fluoromax-P fluorimeter. Fluorescence micrographs were recorded on an Olympus BX51 widefield microscope (1000×, NA 0.95) equipped with a fluorescence cube (330−385 nm excitation filter, a 400 nm dichroic mirror, and a 420 nm long-pass emission filter) and Hg light illumination. For polarized fluorescence measurements, a polarizing film was placed between the sample and the eyepiece of the microscope. Electron micrographs were obtained on a FEI XL30-SFEG scanning electron microscope (SEM) or on a Philips CM12 transmission electron microscope (TEM). Samples for SEM were prepared by drop-coating onto 25 mm^2 pieces of a silicon wafer or onto aluminum stubs. Samples

(15) Hikmet, R. A. M.; Chin, P. T. K.; Talapin, T. P. *Adv. Mater.* **2005**, *17*, 1436−1439.
(16) Kim, J. Y.; Osterloh, F. E.; Hiramatsu, H.; Dumas, R. K.; Liu, K. *J. Phys. Chem. B* **2005**, *109* (22), 11151−11157.
(17) Mekis, I.; Talapin, D. V.; Kornowski, A.; Haase, M.; Weller, H. *J. Phys. Chem. B* **2003**, *107*(30), 7454−7462.

for TEM were prepared analogously using holey carbon copper grids (TedPella). Elemental analyses were performed with an EDAX energy-dispersive X-ray spectroscopy (EDS) system.

Synthesis of CdSe−APS−$Ca_2Nb_3O_{10}$ Clusters. APS-ligated $Ca_2Nb_3O_{10}$ nanosheets (5 mg) [16] were dispersed in 5 mL of THF with brief sonication, and a solution of 20 mg of TOPO-ligated CdSe/CdS nanoparticles (5.4 nm) in 1 mL of $CHCl_3$ was quickly added. After 20 min of rapid stirring at room temperature, a red-brown solid formed, which was centrifuged off and washed three times with a total of 50 mL of $CHCl_3$ to remove excess CdSe nanoparticles. The solid was kept together with a few drops of residual $CHCl_3$ in a closed container in the dark. By EDS the mass composition (%) of the clusters is C (12.2), N (4.8), O (15.5), Si (2.7), Nb (21.9), Ca (5.2), Cd (19.9), Se (17.8), suggesting a molecular composition of $Ca_2Nb_3O_{10} \cdot APS \cdot 2.0H_2O \cdot 2.25CdSe \cdot 0.5TOPO$.

Reaction of CdSe-APS−$Ca_2Nb_3O_{10}$ with Oleylamine. CdSe−APS−$Ca_2Nb_3O_{10}$ (5 mg) was dispersed in 10 mL of $CHCl_3$, and 20 mg of oleylamine was slowly added with rapid stirring at room temperature. The mixture was refluxed for 20 min, during which the red emission from CdSe disappeared. The formed solid was centrifuged off and washed with 15 mL of $CHCl_3$. TEM analysis revealed that the solid consisted of $Ca_2Nb_3O_{10}$ nanosheets with greatly reduced CdSe content (Figure S3).

Results and Discussion

Soluble, platelike clusters of CdSe nanocrystals form by reaction of 3-aminopropylsilyl-modified $Ca_2Nb_3O_{10}$ nanosheets with an excess of trioctylphosphine oxide-coated CdSe nanocrystals in THF according to Figure 2. In the reaction, the terminal amine groups on the nanosheets displace the TOPO ligands on the CdSe nanocrystal surface.

Transmission electron micrographs (Figure 3A,B) reveal that the CdSe−$Ca_2Nb_3O_{10}$ clusters consist of $Ca_2Nb_3O_{10}$ nanosheets that are decorated on both sides with 5.4 ± 0.6 nm CdSe particles at a density of 5340 ± 310 CdSe particles per square micrometer per side per single sheet. Some of the CdSe particles on the sheets appear in groups of closely spaced, frequently hexagonally ordered, groups, suggesting that van der Waals interactions between nanocrystals affect the formation of these structures. However, the majority of the CdSe particles are separated by 3.0 ± 0.7 nm, which is consistent with covalent bonding between the nanocrystals and primary amines on the aminopropylsilyl-modified sheets.

According to AFM profile scans (Figure 3D), the thickness of a single-layered CdSe−$Ca_2Nb_3O_{10}$ cluster (17.24 nm) is exactly the sum of two 6−7-nm-thick layers of CdSe particles on both sides of the sheet and the thickness of the sheet itself (2 nm). Due to their planar shape and high surface area, most of these single-layer clusters stack into multilayered clusters with a mean length/width of 3.92 ± 1.18 μm and with
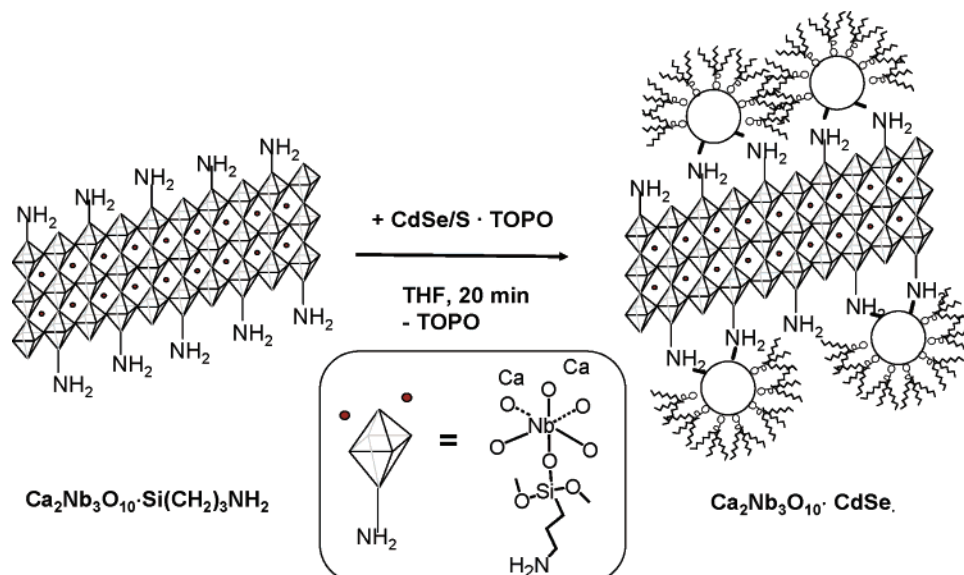
Figure 2. Formation of platelike CdSe nanocrystal clusters. The APS-modifed $Ca_2Nb_3O_{10}$ nanosheet is shown as a projection perpendicular to the sheet plane. The insert shows the structure of the octahedral NbO_6 sites in the sheets and the suggested binding of the silane to the sheets.[16]
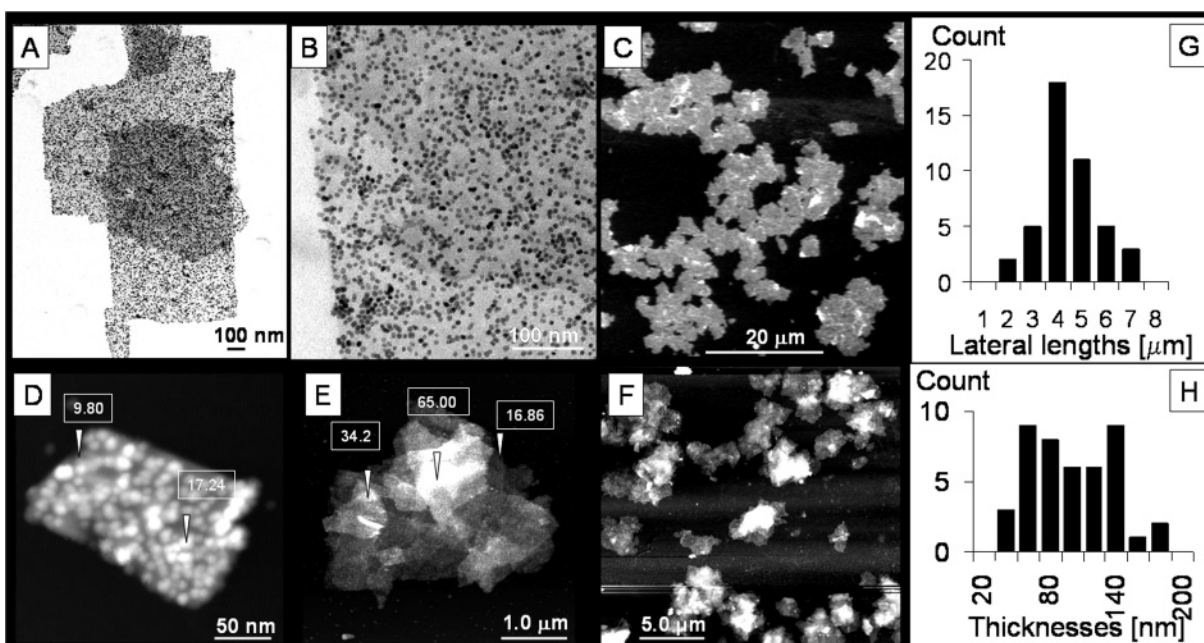

Figure 3. Morphology of CdSe−$Ca_2Nb_3O_{10}$ clusters. (A, B) TEMs of double layer CdSe−$Ca_2Nb_3O_{10}$ clusters, (C) SEM of several multilayer clusters, (D−F) AFMs of single layer cluster (D) and of one (E) and several (F) multilayer clusters. (G, H) Size distributions of clusters. Inserts in D show measured height [nm].

thicknesses of 91 ± 37 nm (distributions in Figure 3G,H). The high aspect ratio (>40) of these structures is due to the flatness of the individual CdSe−$Ca_2Nb_3O_{10}$ building blocks. The structures are very similar to the related Fe_3O_4−$Ca_2Nb_3O_{10}$ clusters, which form analogously by reaction of 3-APS−Ca_2-Nb_3O_{10} with magnetite nanoparticles.[16] Interestingly, the lateral dimensions of the Fe_3O_4−$Ca_2Nb_3O_{10}$ clusters follow a log-normal size distribution,[16] whereas the lateral size distribution for CdSe−$Ca_2Nb_3O_{10}$ is of the Gaussian type (Figure 3G). This suggests two different aggregation mechanisms in these related systems.

X-ray powder diffraction spectra (Figure 4A) demonstrate that the crystalline structure of the CdSe and $Ca_2Nb_3O_{10}$ nanoparticle building blocks is retained in the clusters. The spectrum for the CdSe−$Ca_2Nb_3O_{10}$ clusters contains sharp peaks

for the $Ca_2Nb_3O_{10}$ intrasheet reflections and broad peaks for reflections belonging to the CdSe nanocrystals. The half-width of the 110 peak for CdSe suggests a diameter of 5.8 nm for the nanocrystals (5.4 nm from TEM).[18] Comparison of the spectra of the CdSe−$Ca_2Nb_3O_{10}$ clusters and of 3-APS−$Ca_2Nb_3O_{10}$ shows that the intrasheet reflections (*hk*0) do not broaden upon intercalation of the CdSe nanoparticles. The absence of buckling of sheets is remarkable, considering the almost 3 times larger diameter of CdSe nanocrystals compared to the sheets.

The molecular composition (Experimental Section) of the clusters is $Ca_2Nb_3O_{10} \cdot APS \cdot 2.0H_2O \cdot 2.25CdSe \cdot 0.5TOPO$ according to element dispersive spectroscopy (EDS, Figure S1).

(18) Klug, H. P.; Alexander, L. E. *X-ray diffraction procedures for polycrys-talline and amorphous materials*, 2nd ed.; Wiley: New York, 1974; p xxv, 966.
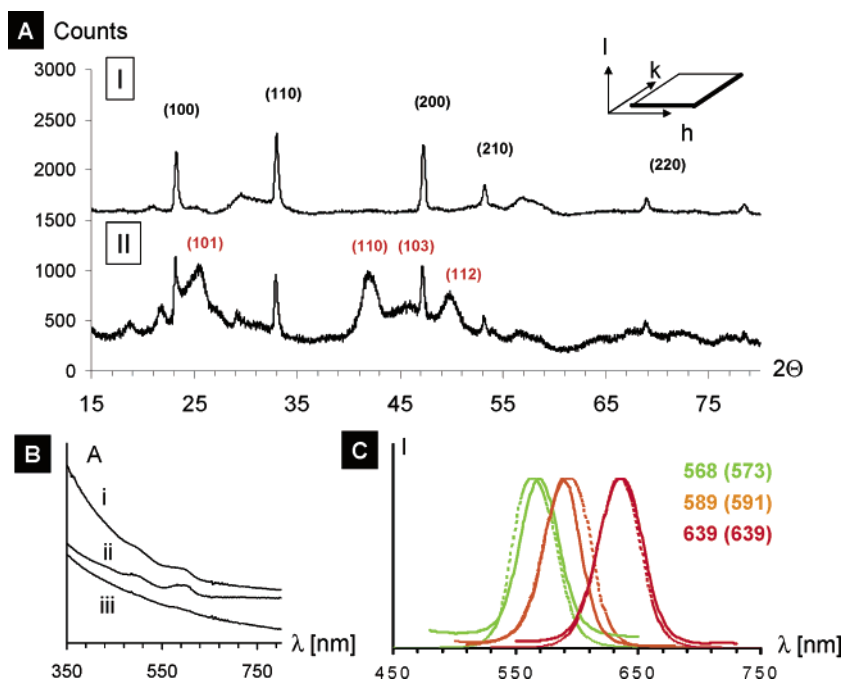
Figure 4. (A) X-ray diffraction patterns of (I) $Ca_2Nb_3O_{10}$–APS (indices are for $Ca_2Nb_3O_{10}$) and (II) CdSe–$Ca_2Nb_3O_{10}$ (indices are for CdSe). (B) UV/vis spectra of (i) CdSe–$Ca_2Nb_3O_{10}$, (ii) CdSe·TOPO, and (iii) $Ca_2Nb_3O_{10}$–APS. (C) Photoluminescence spectra (λ_{exc} = 400 nm) of (i) $Ca_2Nb_3O_{10}$–CdSe and (ii) CdSe·TOPO (broken lines). All spectra were recorded for samples dispersed in THF and were normalized with regard to intensity.

Both water and TOPO ligands also show up in the IR spectra (Figure S2) of the material with intense C–H stretching bands at 2926 cm^{-1} and bands at 3458 and 1638 cm^{-1} for the O–H stretch and bending modes of water. While TOPO is likely still bonded to the CdSe portion of the clusters, the water is likely associated with the hydrophilic Nb–O surface of the nanosheets. The spectra further reveal characteristic bands for Si–O at 1070–1135 cm^{-1}, in agreement with the presence of μ-O bonded APS.

The CdSe–$Ca_2Nb_3O_{10}$ clusters are relatively stable against dissociation, even in coordinating solvents such as pyridine and THF. However, treatment with oleylamine (9-octadecenylamine) in chloroform at 60 °C for 20 min leads to detachment of nanosheets and CdSe nanocrystals (Figure S3). The outcome of this reaction and the chemical inertness of the CdSe–$Ca_2Nb_3O_{10}$ clusters in weakly coordination solvents suggest that the clusters are supported by covalent interactions between Cd ions on the surface of the CdSe nanocystals and amine groups on the sheets.

The optical properties of the CdSe–$Ca_2Nb_3O_{10}$ clusters are characterized by broad featureless absorptions that diminish with increasing wavelength (Figure 4B-i). This absorption reflects a scattering contribution from the nanosheets and the band gap absorption of the CdSe nanocrystals, both components of which can be seen in spectra of the separate components (spectra ii and iii). The absorption component of CdSe terminates at 640 nm with a shoulder characteristic for the 5.4 nm CdSe nanocrystals. Optical excitation at λ_{exc} = 400 nm causes the CdSe–$Ca_2Nb_3O_{10}$ clusters to emit strongly at 568 (green), 589 (orange), 639 (red) nm (Figure 4C), depending on the size of the nanocrystals. Compared to the free CdSe nanocrystals, the emissions occur at the same wavelength and with the same intensity.

To probe the three-dimensional emission characteristics of the nanomaterials, wide field fluorescence micrographs (λ_{exc} = 330–385 nm) were collected on films of clusters with CdSe nanocrystals emitting at 639, 589, and 568 nm on a gold-coated glass slide (Figure 5A–C). In these cases, the clusters are aligned coplanar with the surface of the gold-coated glass substrate.

It can be seen that the light emitted from the clusters is most intense around the edges of individual clusters, whereas the centers remain relatively dark. For some clusters, additional emission patterns are visible near the cluster centers that seem to arise from structural features present at the top of the clusters. The appearance of the micrographs changes, when the clusters are tilted with respect to the viewing direction (Figure 5D–F) so that they can be observed parallel to the cluster plane. The emission patterns now take the form of lines, which by SEM (S-4) can be shown to coincide with edges of the clusters. The fact that the emission from the cluster edges is linearly polarized can be shown by placing a polarizing film between the sample and the eyepiece. Under these conditions, the intensity of the emission from the lines is enhanced or attenuated, depending on the relative orientation of the polarized film (shown as arrows in Figure 5D–F). The polarized and enhanced emission indicates that it arises from a waveguiding process inside the clusters. In contrast, the emission from the cluster centers is not polarized.

The directional emission effect is retained, albeit with reduced efficiency, when the clusters are immersed in a medium with higher index of refraction. The top and bottom images in Figure 5G show the CdSe–$Ca_2Nb_3O_{10}$ clusters in air and under a cover of hydrocarbon oil (n = 1.59), respectively. In the latter case, the fluorescence of the clusters is still most intense near the cluster edges, which demonstrates that waveguiding still occurs, despite the change of the matrix. However, the changed optical appearance of several clusters indicates a change of the light propagation through these structures.
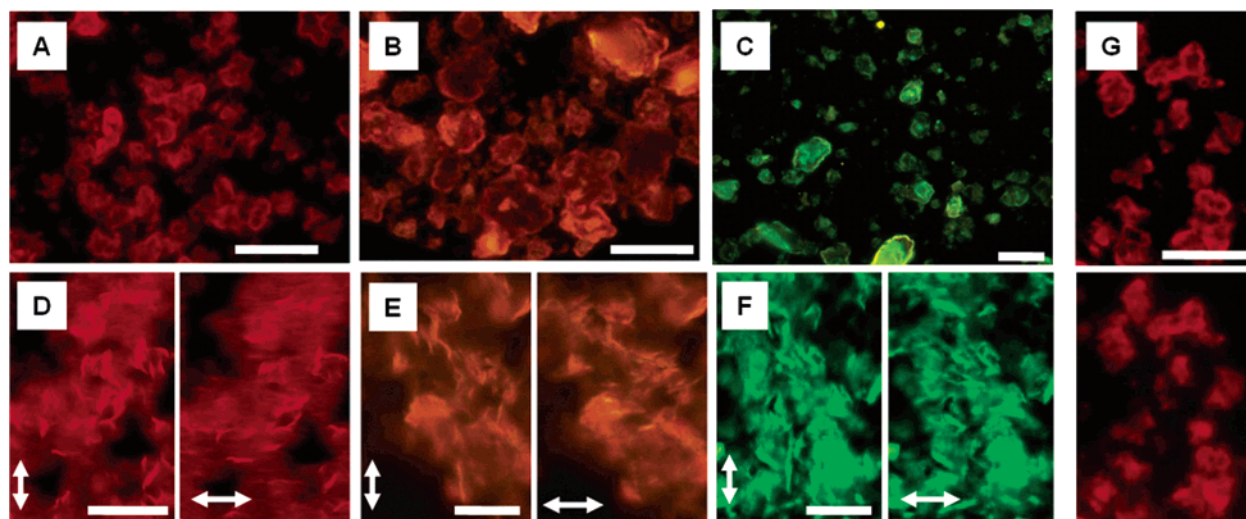
Figure 5. (A−C) Fluorescence micrographs of CdSe−Ca$_2$Nb$_3$O$_{10}$ clusters with red (639 nm), orange (589 nm), or green (568 nm) emission on gold-coated glass slides in air. (D−F) Polarized fluorescence micrographs with analyzer orientation as shown by arrow. (G) Fluorescence of CdSe−Ca$_2$Nb$_3$O$_{10}$ clusters with red (639 nm) emission in air (top) or in hydrocarbon oil ($n = 1.59$, bottom). All scale bars are 10 μm.
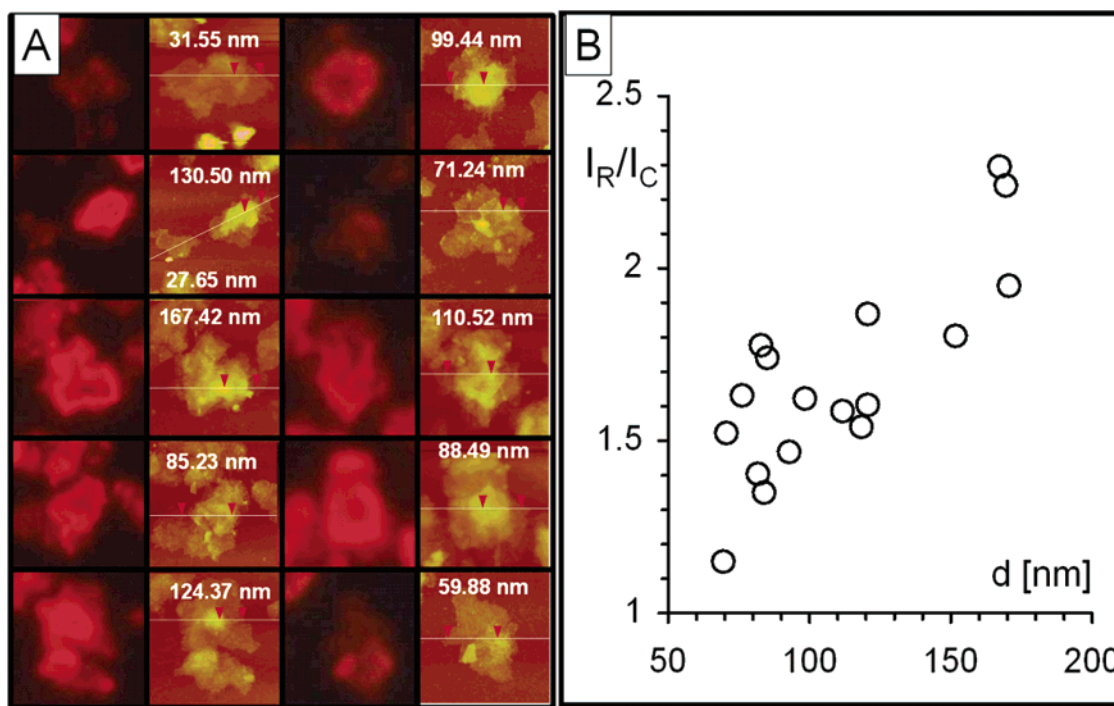

Figure 6. (A) Fluorescence micrographs and AFM scans of the red-emitting CdSe−Ca$_2$Nb$_3$O$_{10}$ clusters on a gold-coated glass slide (scan heights are given in nm). (B) Plot of the directional emission ratio versus the thickness of the clusters. The circle size represents the error of measurement.

To quantify the directional emission from the clusters, and to correlate it with the cluster thickness, AFM surface profile scans were recorded on clusters that had been previously imaged by fluorescence microscopy (FM). The corresponding FM and AFM images are shown in the left and right columns of Figure 6A. The analysis shows that for virtually all measured clusters the directional emission is confined to the top layers of the clusters. The bottom layers, which are in direct contact with the underlying substrate, display no guided emission.

By defining the emission ratio I_R/I_C (with I_R and I_C as the photoemission intensities at the rim and at the centers of the clusters, respectively) and by plotting this ratio against the thickness of the top layers in clusters (Figure 6B), it becomes evident that the directional emission ability of the clusters increases linearly with increasing thickness. This trend is expected from waveguide theory, which predicts increasing optical losses with decreasing feature size of the waveguide.[19] The smallest clusters that show the effect are about 70 nm thick and thus contain about four layers of CdSe−Ca$_2$Nb$_3$O$_{10}$.

In terms of their optical properties, the CdSe−Ca$_2$Nb$_3$O$_{10}$ clusters can be considered as dielectric slab waveguides.[19] In such structures the light propagates along the slab due to total internal reflection at the cluster−air interface. Using the indices of refraction of 2.45 (see below) for the clusters and of 1.0 for the surrounding air, respectively, one calculates 24° as the critical angle for total internal reflection from Snell's law. Planar

(19) Syms, R. R. A.; Cozens, J. R. *Optical guided waves and devices*. McGraw-Hill: London; New York, 1992; p ix, 498.

light waves that approach the cluster–air interface at a greater angle will be reflected back into the cluster, whereas light at a smaller angle will be refracted into the surrounding medium. The fact that in an optically denser hydrocarbon environment ($n = 1.59$) the critical angle increases to 41° is responsible for reduced directional emission of the clusters under those conditions.

On the basis of their thickness (70–160 nm), the cutoff frequency for the waveguides should be 140–320 nm, i.e., light of greater wavelength should not be able to propagate in these structures. From this perspective, the observation of waveguided emission in the $CdSe-Ca_2Nb_3O_{10}$ clusters is unexpected. The enhanced planar waveguiding properties of the clusters are likely related to the structural and compositional characteristics of these materials. First, the refractive indices of $Ca_2Nb_3O_{10}$ (2.49 for Nb_2O_5)[20] and of CdSe (2.45)[21] are high compared to other optically transparent materials. Second, as molecular fragments of the Dion–Jacobsen phase $KCa_2Nb_3O_{10}$, exfoliated $Ca_2Nb_3O_{10}$ sheets are atomically flat (see AFM scans in Figure S5). The small surface roughness of these sheets minimizes scattering losses along the interface and maximizes reflection. These properties and the layered structure of the $CdSe-Ca_2Nb_3O_{10}$ stacks are expected to facilitate the directional and polarized emission of the clusters.

Conclusion

In conclusion, we have demonstrated that the three-dimensional emission characteristics of CdSe nanocrystals can be adjusted by incorporating the nanocrystals into soluble pseudo-two-dimensional microclusters. When excited with UV light, such clusters emit linearly polarized light of tunable wavelength along the cluster plane. The effect is likely due to total internal reflection of light at the cluster/medium interface and can be observed in structures <100 nm thick and in media with a refractive index of up to ~1.6. Because of their directional emission properties, the CdSe clusters might be of interest as optical probes that could provide spatial and orientational information about their environment or as components in materials with direction-dependent optical properties.

Supporting Information Available: EDS and IR spectra of $CdSe-Ca_2Nb_3O_{10}$, TEM images of $CdSe-Ca_2Nb_3O_{10}$ after reaction with oleylamine, SEM image of a $CdSe-Ca_2Nb_3O_{10}$ film, and AFM scans of $Ca_2Nb_3O_{10}$ sheets. This material is available free of charge via the Internet at http://pubs.acs.org.

JA0541377

(20) Nystrom, M. J.; Wessels, B. W.; Studebaker, D. B.; Marks, T. J.; Lin, W. P.; Wong, G. K. *Appl. Phys. Lett.* **1995**, *67* (3), 365–367.
(21) Reck, J.; Beck, U.; Dohrmann, J. K. *Z. Phys. Chem.* **2000**, *214*, 83–93.